

- Inter.* **86**, 45 (1994); Y. Wang, R. C. Liebermann, D. Cuny, L. Galoisy, *Eos* **75**, 613 (1994).
12. See, for example, Y. Wang, F. Guyot, A. Yeganeh-Haeri, R. C. Liebermann, *Science* **248**, 468 (1990).
  13. R. W. G. Wyckoff, *Crystal Structures* (Interscience, New York, ed. 2, 1965), vol. 3. For earlier speculation of  $K_2NiF_4$ -structured  $(Mg,Fe)_2SiO_4$ , see, for example, A. E. Ringwood and A. F. Reid, *Earth Planet. Sci. Lett.* **5**, 67 (1968).
  14. J. P. Poirier, in *Anelasticity in the Earth*, F. D. Stacey, M. S. Patterson, A. Nicholas, Eds. (Geodynamics Series 4, American Geophysical Union, Washington, DC, 1981), pp. 113–117.
  15. D. C. Rubie, *Nature* **308**, 505 (1984); E. Ito and H. Sato, *ibid.* **351**, 140 (1991).
  16. Y. Wang, F. Guyot, R. C. Liebermann, *J. Geophys. Res.* **97**, 12327 (1992); I. Martinez, Y. Wang, F. Guyot, R. C. Liebermann, J. C. Doukhan, *ibid.*, in press.
  17. C.-M. Sung and R. G. Burns, *Tectonophysics* **31**, 1 (1976). Coincidentally, their rate equations predicted a blocking temperature of 973 K for the olivine-spinel

transformation.

18. D. C. Rubie and C. R. Ross II, *Phys. Earth Planet. Inter.* **86**, 223 (1994).
19. The Stony Brook High Pressure Laboratory is jointly supported by the State University of New York at Stony Brook and the NSF Science and Technology Center for High Pressure Research (EAR 89-20239) and by NSF grant EAR 93-04502. Mineral Physics Institute contribution 183.

3 September 1996; accepted 21 November 1996

## Transformation in Garnet from Orthorhombic Perovskite to $LiNbO_3$ Phase on Release of Pressure

Nobumasa Funamori, Takehiko Yagi, Nobuyoshi Miyajima, Kiyoshi Fujino

High-pressure in situ x-ray diffraction and transmission electron microscopy on quenched samples show that natural garnet transforms to orthorhombic perovskite (and minor coexisting phases) containing increasing amounts of aluminum with increasing pressure. This suggests that the perovskite is the dominant host mineral for aluminum in Earth's lower mantle. Orthorhombic perovskite is quenched from ~35 gigapascals but, because of the increased aluminum content, transforms to the  $LiNbO_3$  structure upon quenching from ~60 gigapascals.

In 1974, Liu (1) reported the transformation of a natural garnet, the host mineral of Al in Earth's upper mantle, into the orthorhombic perovskite structure at 30 GPa. Since then, the transformation of garnets of various compositions has been investigated to clarify the host mineral of Al in the lower mantle. The results, however, are complicated and the host remains uncertain, whereas the hosts of the other main cations (Mg, Si, and Fe) in the mantle— $(Mg,Fe)SiO_3$  orthorhombic perovskite and  $(Mg,Fe)O$  magnesiowüstite—are well identified. Weng *et al.* (2) carried out experiments on pyrope ( $Mg_3Al_2Si_3O_{12}$ )—grossular ( $Ca_3Al_2Si_3O_{12}$ ) garnet at 40 GPa and suggested that it transforms to an assemblage of orthorhombic perovskite and unquenchable Ca-rich perovskite. O'Neill and Jeanloz (3) reported the coexistence of garnet with orthorhombic perovskite up to 50 GPa in a pyrope-almandine ( $Fe_3Al_2Si_3O_{12}$ ) system. Irifune *et al.* (4) found the decomposition of pyrope into a sub-aluminous (Al-deficient relative to garnet) orthorhombic perovskite and a corundum-ilmenite solid solution at pressures greater than 26.5 GPa. They also found an increase of Al in the perovskite phase with increasing pressure, and predicted the formation of an aluminous perovskite with pyrope composition above 30 to 40 GPa. Recently, Kesson *et al.* (5) reported

that rhombohedral perovskite, rather than orthorhombic perovskite, is the stable phase of pyrope-almandine garnet at 55 to 70 GPa. On the other hand, Ahmed-Zaid and Madon (6) suggested, from their experiments at 40 to 50 GPa, that the main host mineral of Al varies depending on chemical composition, pressure, and temperature. The candidates they proposed are  $(Ca,Mg,Fe)Al_2Si_2O_8$  with the hollandite structure,  $Al_2SiO_5$  with the  $V_3O_5$  structure, and  $(Ca,Mg)Al_2SiO_6$  with an unknown structure.

To clarify the host mineral of Al under lower mantle conditions, we carried out high-pressure in situ x-ray diffraction experiments on natural garnet with the use of a diamond anvil cell and synchrotron radiation (7). Garnet from the Udachnaya kimberlite pipe in the Sakha Republic (8) with the composition  $Py_{49}Alm_{29}Gro_{21}Sp_1$  [Py, pyrope; Alm, almandine; Gro, grossular; Sp, spessartine ( $Mn_3Al_2Si_3O_{12}$ )] was ground to a powder and used as the starting material. The samples were heated by a yttrium-aluminum-garnet (YAG) laser at two different pressures (9). The recovered samples were examined by transmission electron microscopy (TEM) (10).

The sample was compressed to 67.5 GPa and heated by the YAG laser. Pressure decreased to 52.8 GPa, measured after heating. The x-ray diffraction profile (Fig. 1A) obtained after heating shows that most of the intense lines can be indexed as orthorhombic perovskite, with intensities similar

to those of  $MgSiO_3$  perovskite (11). Unit cell parameters of this phase are  $a = 4.539(4)$  Å,  $b = 4.761(5)$  Å,  $c = 6.622(5)$  Å, and  $V = 143.1(2)$  Å<sup>3</sup>. The other lines can be assigned to Ca-rich perovskite, stishovite, and garnet. A trace amount of stishovite is often observed as a metastable phase during transformation, but it is not clear whether the stishovite observed in this sample is the metastable phase (12). The garnet may be a residual of the starting material that has not been heated to a high enough temperature (9, 13). The orthorhombic perovskite phase was observed on decompression down to 9.6 GPa, although splitting of the characteristic triplet 020+112+200 became unclear with decreasing pressure (Fig. 1, B and C). Both a decrease of the orthorhombic distortion from cubic symmetry (14) and an increase of the pressure gradient across the sample during decompression can explain this phenomenon. Diffraction from the orthorhombic perovskite is not observed in the profile obtained after complete decompression (Fig. 1D). The main peaks can be indexed on the basis of rhombohedral symmetry

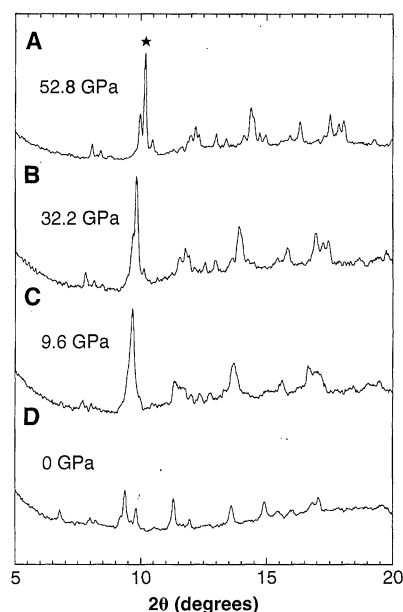


Fig. 1. X-ray diffraction profiles of the ~60 GPa sample obtained during decompression at room temperature. The star indicates the characteristic triplet 020+112+200 of orthorhombic perovskite.

N. Funamori and T. Yagi, Institute for Solid State Physics, University of Tokyo, Minato-ku 106, Japan.  
N. Miyajima and K. Fujino, Department of Earth and Planetary Sciences, Hokkaido University, Sapporo 060, Japan.

(Table 1) and the other lines can be assigned to stishovite and garnet. The low intensities of the peaks of the rhombohedral phase may be attributable to the partial amorphization of orthorhombic perovskite, in addition to amorphization of Ca-rich perovskite. On the other hand, diffraction from orthorhombic perovskite was observed after complete decompression for the sample heated at 39.5 GPa (pressure after heating was 30.2 GPa). In this run, we observed unidentified diffraction lines in addition to those from Ca-rich perovskite (unquenchable), stishovite, and garnet. However, we could not identify the additional phase from the x-ray diffraction profile, because these lines are weak and many of them overlap with lines from the other phases.

TEM observation on the sample recovered from ~60 GPa revealed that the rhombohedral phase has a composition close to that of the starting material but deficient in CaSiO<sub>3</sub>. This phase exhibits a lamellar-twinning microstructure, and all the twin planes examined were {101̄2} (Fig. 2). The orthorhombic perovskite recovered from the ~35 GPa experiment is deficient in Al<sub>2</sub>O<sub>3</sub> relative to the rhombohedral phase (and the starting material). Only a negligible amount (< ~1 weight %) of the Al-rich phase was observed in the ~60 GPa sample, which agrees with the x-ray observation, whereas a small but significant amount (~10 weight %) was observed in the ~35 GPa sample. The chemical composition of the Al-rich phase in the ~60 GPa sample is close to that in the ~35 GPa sample. This Al-rich phase may correspond to the unidentified x-ray diffraction lines observed in the ~35 GPa experiment. Electron diffraction patterns taken on the Al-rich phase cannot be indexed on the basis of a corundum-ilmenite solid solution (4). Although the chemical composition of the Al-rich phase has not been determined definitively, it is close to (Ca,Mg,Fe)Al<sub>2</sub>SiO<sub>6</sub> (6) but enriched in (Ca,Mg,Fe)O and deficient in SiO<sub>2</sub>, and it differs from (Ca,Mg,Fe)Al<sub>2</sub>Si<sub>2</sub>O<sub>8</sub> (6) or Al<sub>2</sub>SiO<sub>5</sub> (6).

**Table 1.** Observed and calculated x-ray diffraction pattern of the rhombohedral phase at ambient conditions.

| <i>h</i> | <i>k</i> | <i>l</i> | <i>d</i> <sub>obs</sub> | <i>d</i> <sub>calc</sub> * | <i>d</i> <sub>obs</sub> / <i>d</i> <sub>calc</sub> - 1 |
|----------|----------|----------|-------------------------|----------------------------|--|
| 0        | 1        | 2        | 3.5001                  | 3.4993                     | 0.0002   |
| 1        | 0        | 4        | 2.5340                  | 2.5345                     | -0.0002  |
| 1        | 1        | 0        | 2.4183                  | 2.4183                     | 0.0000   |
| 1        | 1        | 3        | 2.1033                  | 2.1012                     | 0.0010   |
| 2        | 0        | 2        | 1.9897                  | 1.9895                     | 0.0001   |
| 0        | 2        | 4        | 1.7485                  | 1.7496                     | -0.0006  |
| 1        | 1        | 6        | 1.5953                  | 1.5951                     | 0.0001   |
| 0        | 3        | 0        | 1.3962                  | 1.3962                     | 0.0000   |

\**a* = 4.837(1) Å, *c* = 12.733(7) Å, *V* = 258.0(2) Å<sup>3</sup> (hexagonal axis).

The rhombohedral phase observed in the recovered ~60 GPa sample seems to be identical to "rhombohedral perovskite" observed by Kesson *et al.* (5), because of the similarities of the experimental conditions and the results of TEM observations (lamellar-twinning microstructure and chemical composition). However, we interpret this phase as having the LiNbO<sub>3</sub> structure. Candidate structures include (i) rhombohedral perovskite, (ii) corundum, (iii) ilmenite, and (iv) LiNbO<sub>3</sub>. Among them, corundum can be rejected because it has a different chemical composition. The rhombohedral phase has a composition close to the starting material. The *c/a* ratio of this phase is 2.63, whereas it is 2.87 for MgSiO<sub>3</sub> ilmenite (15); therefore, it is also unlikely to have ilmenite structure. The Goldschmidt tolerance factor  $t = (1/2)^{1/2}(r_A + r_O)/(r_B + r_O)$ , where *r*<sub>A</sub>, *r*<sub>B</sub>, and *r*<sub>O</sub> are the ionic radii of the A-site cation, B-site cation, and oxygen anion, respectively, is useful for discussing the perovskite-structured compounds by systematics (16). Neglecting Fe, Ca, and Mn for simplicity, we obtain *t* = 0.83 for Mg<sub>4</sub>Si<sub>4</sub>O<sub>12</sub> and *t* = 0.80 for Mg<sub>3</sub>Al<sub>2</sub>Si<sub>3</sub>O<sub>12</sub>. Ionic radii in sixfold coordination from Shannon and Prewitt (17) were used in the calculation. Rhombohedral perovskite is unlikely, because this phase is usually formed when *t* > ~0.85. MnTiO<sub>3</sub> forms orthorhombic perovskite structure at high pressure and transforms to LiNbO<sub>3</sub> structure during decompression (18). The value of *t* for MnTiO<sub>3</sub> is 0.79, which is

close to that for Mg<sub>3</sub>Al<sub>2</sub>Si<sub>3</sub>O<sub>12</sub>. Similar transformations have also been observed in Mn-SnO<sub>3</sub> (16), FeTiO<sub>3</sub> (16), and MgGeO<sub>3</sub> (19), where *t* = 0.75 to 0.77. The increase of Al in the perovskite phase with increasing pressure reduces *t* and may cause the transformation to the LiNbO<sub>3</sub> phase (20). The sub-aluminous perovskite coexisting with the Al-rich phase at ~35 GPa did not transform to this phase. A twinned microstructure, such as that observed in our ~60 GPa sample, was also reported for MnTiO<sub>3</sub> (21) and MgGeO<sub>3</sub> (19). The orientation of twin planes is the same for all three materials. This coincidence supports our conclusion that the aluminous orthorhombic perovskite transforms to LiNbO<sub>3</sub> during decompression.

Our results show that the capacity of orthorhombic perovskite to accommodate Al increases with pressure. Because experiments on model mantle rock suggest that orthorhombic perovskite accommodates the mantle inventory of Al even at the conditions of the uppermost part of the lower mantle (22), this phase seems to be the host mineral of Al, at least in the upper half of the lower mantle. This conclusion is compatible with the results of the experiment on natural rock conducted at 54 GPa (23).

## REFERENCES AND NOTES

- L. G. Liu, *Geophys. Res. Lett.* **1**, 277 (1974).
- K. Weng, H. K. Mao, P. M. Bell, *Carnegie Inst. Washington Year Book* **81**, 273 (1982).
- B. O'Neill and R. Jeanloz, *J. Geophys. Res.* **99**, 19901 (1994).
- T. Irifune, T. Koizumi, J. Ando, *Phys. Earth Planet. Inter.* **96**, 147 (1996).
- S. E. Kesson, J. D. Fitz Gerald, J. M. G. Shelley, R. L. Withers, *Earth Planet. Sci. Lett.* **134**, 187 (1995).
- I. Ahmed-Zaid and M. Madon, *ibid.* **129**, 233 (1995).
- The angle-dispersive x-ray diffraction study was carried out at BL13B2 of the National Laboratory for High Energy Physics (KEK), Japan. Monochromatized x-rays ( $\lambda = 0.4143$  Å) and an imaging-plate detector [J. Miyahara *et al.*, *Nucl. Instrum. Methods* **A246**, 572 (1986)] were used in the experiments.
- N. V. Sovolev *et al.*, in *Kimberlites of Yakutia (Field Guide Book)*, Sixth International Kimberlite Conference (ALMAZY Rossi-SAKHA, United Institute of Geology, Geophysics, and Mineralogy, Novosibirsk, 1995), pp. 60-73.
- Laser light ( $\lambda = 1.06$  μm) was focused to a diameter of ~15 μm and was scanned to heat the entire sample (diameter ~120 μm). The total heating duration was ~60 min for both runs. Maximum temperature is expected to have been below the melting temperature, ~3000 K (24) [A. Zerr and R. Boehler, *Science* **262**, 553 (1993)], because neither visual observations during heating nor TEM observations on recovered samples gave any indication of melting. Also, the maximum temperature is likely to have been above ~1800 K, because Irifune *et al.* (4) observed a residual garnet at 1800 K. Pressure was measured by the ruby fluorescence technique [H. K. Mao *et al.*, *J. Appl. Phys.* **49**, 3276 (1978)]. To reduce possible contamination, we placed a small ruby chip (diameter ~5 μm) at the midpoint between the center and the edge of the sample to measure an average pressure. The pressure during heating is expected to have been higher than the pressure measured after heating because of thermal pressure (24).
- The samples were ion-thinned with the use of a cooling stage to prevent thermal damage. A 200-kV

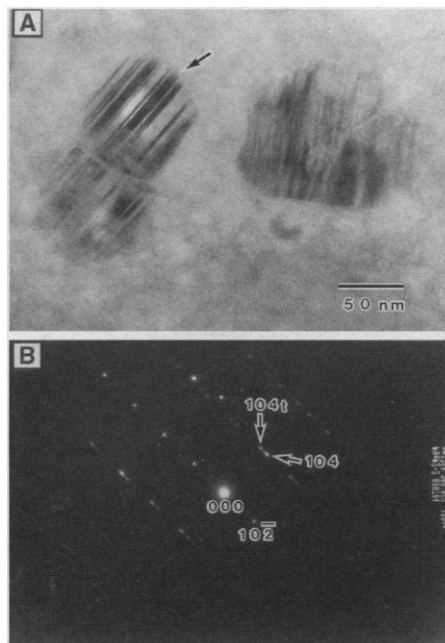


**Fig. 2.** (A) TEM micrograph of the sample recovered from ~60 GPa. (B) Selected area electron diffraction pattern of the grain indicated by the arrow in (A). The grain shows the polysynthetic twinning on the plane {101̄2}.

- JEM-2010 analytical transmission electron microscope was used. Detailed TEM observations of these and other samples are reported elsewhere (N. Miyajima *et al.*, in preparation).
- E. Ito and Y. Matsui, *Earth Planet. Sci. Lett.* **38**, 443 (1978); T. Yagi, H. K. Mao, P. M. Bell, *Phys. Chem. Miner.* **3**, 97 (1978).
  - We often observe stishovite even for enstatite ( $\text{MgSiO}_3$ ) heated by the YAG laser, which is known to transform to the single phase of perovskite. It is also observed in our multi-anvil experiments, in which the heating duration is 1 to 2 min at  $\sim 1800$  K, but it usually disappears by heating for 30 min or more at the same temperature.
  - The x-ray diffraction lines of the garnet are broad compared with those of the other phases, indicating the presence of unrelaxed stress. The unit cell parameter of the recovered garnet is the same as that of the starting material within experimental uncertainty. In addition, the garnet has not been observed by TEM, probably because the low-temperature part of the sample, which had been adjacent to diamonds, was removed during ion-thinning. From these observations, we believe that the garnet observed after heating is residual starting material.
  - H. K. Mao *et al.*, *J. Geophys. Res.* **96**, 8069 (1991); N. Funamori, T. Yagi, T. Uchida, W. Utsumi, *Proc. 14th AIRAPT Conf.*, 791 (1994).
  - L. G. Liu, *Earth Planet. Sci. Lett.* **31**, 200 (1976); E. Ito and Y. Matsui, in *High-Pressure Research: Applications in Geophysics*, M. H. Manghni and S. Akimoto, Eds. (Academic Press, New York, 1977), pp. 193–208.
  - K. Leinenweber, W. Utsumi, Y. Tsuchida, T. Yagi, K. Kurita, *Phys. Chem. Miner.* **18**, 244 (1991).
  - R. D. Shannon and C. T. Prewitt, *Acta. Crystallogr. B* **26**, 925 (1969).
  - N. L. Ross, J. Ko, C. T. Prewitt, *Phys. Chem. Miner.* **16**, 621 (1989).
  - K. Leinenweber, Y. Wang, T. Yagi, H. Yusa, *Am. Mineral.* **79**, 197 (1994).
  - The orthorhombic perovskite with  $\text{Ca}_3\text{Al}_2\text{Si}_3\text{O}_{12}$  composition transforms to amorphous phase on release of pressure [H. Yusa *et al.*, *Phys. Earth Planet. Inter.* **92**, 25 (1995)]. Although the  $t$  value of  $\text{Ca}_3\text{Al}_2\text{Si}_3\text{O}_{12}$  (0.88) is smaller than that of  $\text{Ca}_3\text{Si}_4\text{O}_{12}$  (0.94), it is still very large because of the large radius of  $\text{Ca}^{2+}$ .
  - J. Ko and C. T. Prewitt, *Phys. Chem. Miner.* **15**, 355 (1988).
  - T. Irfune, *Nature* **370**, 131 (1994).
  - B. O'Neill and R. Jeanloz, *Geophys. Res. Lett.* **17**, 1477 (1990).
  - D. L. Heinz and R. Jeanloz, *J. Geophys. Res.* **92**, 11437 (1987).
  - We thank O. Shimomura, T. Kikegawa, K. Aoki, H. Fujihisa, H. Yamawaki, T. Kondo, T. Uchida, and M. Yamakata for support of the experiments and R. Jeanloz, M. Akaogi, and C. T. Prewitt for helpful comments. The garnet sample was provided by T. Watanabe and A. Agashev. X-ray experiments were carried out at KEK (96S02). N.F. and N.M. were supported by Research Fellowships of the Japan Society for the Promotion of Science for Young Scientists.

30 July 1996; accepted 10 December 1996

## An $\text{Fe}_2^{\text{IV}}\text{O}_2$ Diamond Core Structure for the Key Intermediate Q of Methane Monooxygenase

Lijin Shu, Jeremy C. Nesheim, Karl Kauffmann, Eckard Münck, John D. Lipscomb, Lawrence Que Jr.\*

A new paradigm for oxygen activation is required for enzymes such as methane monooxygenase (MMO), for which catalysis depends on a nonheme diiron center instead of the more familiar Fe-porphyrin cofactor. On the basis of precedents from synthetic diiron complexes, a high-valent  $\text{Fe}_2(\mu\text{-O})_2$  diamond core has been proposed as the key oxidizing species for MMO and other nonheme diiron enzymes such as ribonucleotide reductase and fatty acid desaturase. The presence of a single short Fe–O bond (1.77 angstroms) per Fe atom and an Fe–Fe distance of 2.46 angstroms in MMO reaction intermediate Q, obtained from extended x-ray absorption fine structure and Mössbauer analysis, provides spectroscopic evidence that the diiron center in Q has an  $\text{Fe}_2^{\text{IV}}\text{O}_2$  diamond core.

The MMO enzyme system found in methanotrophic bacteria initiates the oxidation of methane (1, 2), thereby preventing the atmospheric egress of nearly 1 billion tons of this greenhouse gas annually. MMO catalyzes the difficult oxidation of methane ( $\text{CH}_4$ ) to methanol ( $\text{CH}_3\text{OH}$ ) with incorporation of one oxygen atom from  $\text{O}_2$ . The

soluble MMO system consists of three separate protein components termed the hydroxylase (MMOH), reductase (MMOR), and component B (MMOB) (3, 4). The crystal structures of MMOH have revealed a nonheme diiron active site (5–7) where oxygen activation and substrate oxidation occur (4). Transient kinetic analysis of a single-turnover reaction has revealed at least five and probably six intermediates in the catalytic cycle, among which intermediate Q is the key oxidizing species (8–11). The Mössbauer properties of Q indicate an exchange-coupled high-valent  $\text{Fe}^{\text{IV}}\text{Fe}^{\text{IV}}$  cluster. The  $\text{Fe}^{\text{IV}}$  oxidation state has been assigned on the basis of the large decrease in isomer shift from  $\delta = 0.50$  mm  $\text{s}^{-1}$  for  $\text{Fe}^{\text{III}}\text{Fe}^{\text{III}}$  MMOH to  $\delta = 0.17$  mm  $\text{s}^{-1}$  for Q

**Table 1.** Compositions of freeze-quenched EXAFS samples of MMOH intermediate Q determined by Mössbauer spectroscopy. An optimal time window from 100 to 320 ms, determined by stopped-flow spectroscopy at  $17^\circ\text{C}$ , was used to quench a single-turnover reaction and trap intermediate Q according to the experimental procedure reported previously (8, 9, 12). Sample 1 was trapped at 150 ms and sample 2 was trapped at 300 ms, allowing us to study two samples with different concentrations of Q for comparison of their EXAFS feature intensities.

| Sample | $\text{Fe}^{\text{II}}\text{Fe}^{\text{II}}$ form | Intermediate P | Intermediate Q | $\text{Fe}^{\text{III}}\text{Fe}^{\text{III}}$ form |
|--------|---|----------------|----------------|---|
| 1      | 27%   | 5%             | 61%            | 7%  |
| 2      | 33%   | 5%             | 44%            | 18%*  |

\*Samples 1 and 2 both have a contribution from  $\text{Fe}^{\text{III}}\text{Fe}^{\text{III}}$  MMOH. The spectrum of sample 2 revealed an additional species with parameters similar to those of the oxo-bridged  $\text{Fe}^{\text{III}}\text{Fe}^{\text{III}}$  cluster of ribonucleotide reductase. We have seen this component in various samples prepared to trap intermediates of the MMOH cycle.

(12); the latter value is comparable to the  $\delta$  values for well-characterized  $\text{Fe}^{\text{IV}}$  complexes (13, 14). To date, no high-valent intermediate of any metalloxygenase has been structurally characterized. Here, we report extended x-ray absorption fine structure (EXAFS) studies of *Methylosinus trichosporium* OB3b MMOH intermediate Q that provide spectroscopic evidence that an enzyme uses an  $\text{Fe}_2(\mu\text{-O})_2$  diamond core for alkane oxidation (15).

A rapid freeze-quench technique allowed us to trap Q in the optimal time domain after mixing  $\text{Fe}^{\text{II}}\text{Fe}^{\text{II}}$  MMOH with 100%  $\text{O}_2$ -saturated buffer in the presence of two equivalents of MMOB (8, 9, 12). The samples were analyzed by Mössbauer spectroscopy to provide an independent quantitation of the reaction cycle intermediates in the samples before and after the x-irradiation inherent in the EXAFS experiment. Figure 1 shows a 4.2 K Mössbauer spectrum of Q sample 1 and the corresponding features that make up this spectrum. The progressive decrease in isomer shift  $\delta$  upon passage through successive reaction cycle intermediates  $\text{Fe}^{\text{II}}\text{Fe}^{\text{II}}$  MMOH, P (16), and Q indicates the increasing oxidation state of the two Fe sites. The Mössbauer-determined compositions of the two freeze-quenched samples 1 and 2 are listed in Table 1. As indicated, intermediate Q represented substantial fractions of each sample, 61% and 44%, respectively; these percentages were the same before and after irradiation.

The R-space EXAFS spectra of four MMOH samples (17) have features that correspond to the distances from each Fe site to surrounding atoms (Fig. 2). For example, the  $\text{Fe}^{\text{II}}\text{Fe}^{\text{II}}$  MMOH sample shows one prominent feature at  $R \sim 2.1$  Å (Fig.

L. Shu and L. Que Jr., Department of Chemistry and Center for Metals in Biocatalysis, University of Minnesota, Minneapolis, MN 55455, USA.

J. C. Nesheim and J. D. Lipscomb, Department of Biochemistry, Medical School, and Center for Metals in Biocatalysis, University of Minnesota, Minneapolis, MN 55455, USA.

K. Kauffmann and E. Münck, Department of Chemistry, Carnegie Mellon University, Pittsburgh, PA 15213, USA.

\*To whom correspondence should be addressed. E-mail: QUE@chem.umn.edu